THE JOURNAL OF BIOLOGICAL CHEMISTRY VOL. 282, NO. 40, pp. 29621–29633, October 5, 2007

Diffusion and Not Active Transport Underlies and Limits ERK1/2 Synapse-to-Nucleus Signaling in Hippocampal Neurons*[S]

Received for publication, February 20, 2007, and in revised form, August 1, 2007 Published, JBC Papers in Press, August 3, 2007, DOI 10.1074/jbc.M701448200

J. Simon Wiegert, C. Peter Bengtson, and Hilmar Bading[1]

From the Department of Neurobiology, Interdisciplinary Center for Neurosciences, University of Heidelberg, 69120 Heidelberg, Germany

The propagation of signals from synapses and dendrites to the nucleus is crucial for long lasting adaptive changes in the nervous system. The ERK-MAPK pathway can link neuronal activity and cell surface receptor activation to the regulation of gene transcription, and it is often considered the principal mediator of synapse-to-nucleus communication in late-phase plasticity and learning. However, the mechanisms underlying ERK1/2 trafficking in dendrites and nuclear translocation in neurons remain to be determined leaving it unclear whether ERK1/2 activated at the synapse can contribute to nuclear signaling and transcriptional regulation. Using the photobleachable and photoactivable fluorescent tag Dronpa on ERK1 and ERK2, we show here that ERK1/2 translocation to the nucleus of hippocampal neurons is induced by the stimulation of *N*-methyl-D-aspartate receptors or TrkB stimulation and is apparently mediated by facilitated diffusion. In contrast, ERK1/2 trafficking within dendrites is not signal-regulated and is mediated by passive diffusion. Within dendrites, the reach of a locally activated pool of ERK1/2 is very limited and follows an exponential decay with distance. These results indicate that successful signal propagation to the nucleus by the ERK-MAPK pathway depends on the distance of the nucleus from the site of ERK1/2 activation. ERK1/2 activated within or near the soma may rapidly reach the nucleus to induce gene expression, whereas ERK1/2 activated at distal synapses may only contribute to local signaling.

The extracellular signal-regulated kinase/mitogen-activated protein (ERK-MAP)[2] kinase cascade is a multifunctional signaling module that plays an important role in the development, differentiation, and proliferation of many cell types. In the nervous system, ERK1 and ERK2 are activated by trophic factors, such as BDNF (1) and electrical activity causing calcium influx into neurons through NMDA receptors or voltage-gated calcium channels (2, 3). A large body of literature has implicated the ERK-MAP kinase pathway in numerous activity-driven neuronal processes, including neuronal survival, synaptic plasticity and learning (4, 5), circadian rhythms (6), pain (7), and addiction (8). ERK1/2 can act locally near the site of activation by cell surface receptors or ion channels to control, for example, the trafficking of α-amino-3-hydroxy-5-methyl-4-isoxazolepropionic acid receptors (9). Another putative role of ERK1/2 in the nervous system is to propagate signals generated at the synapse along the dendrites toward and into the cell nucleus, where it leads to induction of gene transcription. ERK1/2 can phosphorylate several transcription factors, including the ternary complex factors Elk-1 (10, 11) and SAP-1/2 (12), as well as c-Jun (13) and c-Fos (14). The cAMP-response element-binding protein (CREB) is also a target of the ERK-MAP kinase pathway, although CREB phosphorylation on its activator site serine 133 is catalyzed not by ERK1/2 but by the ERK1/2-regulated kinases ribosomal protein S6 kinase 2 and mitogen- and stress-activated protein kinase 1 (MSK1) (15–18).

Despite the evidence for ERK1/2 functions in neuronal signal propagation and gene regulation in the brain, little is known about the mechanisms that mediate trafficking and nuclear translocation of ERK1/2 in neurons. To phosphorylate transcription factors, ERK1/2 have to propagate to the cell nucleus from the site of activation, which in the case of synaptic activity is the submembranous space in the immediate vicinity of synaptic NMDA receptors (19). Long distance communication may be accomplished by active transport or a diffusion process, but it could also involve signaling endosomes, similar to what has been described for nerve growth factor-induced retrograde ERK1/2 signaling in axons (20–22). It is also possible that ERK1/2 activated at the synapse remain spatially confined, acting only locally. In this scenario gene induction only takes place if neuronal activity triggers a burst of action potentials causing global activation of ERK1/2 throughout the neuron, which sub-

* This work was supported by the Alexander von Humboldt Foundation, SFB488, the European Union Network of Excellence NeuroNE, and European Union Project GRIPANNT. The costs of publication of this article were defrayed in part by the payment of page charges. This article must therefore be hereby marked "*advertisement*" in accordance with 18 U.S.C. Section 1734 solely to indicate this fact.

[S] The on-line version of this article (available at http://www.jbc.org) contains supplemental Figs. 1–5.

[1] To whom correspondence should be addressed. Tel.: 496221-54-8218; E-mail: Hilmar.Bading@uni-hd.de.

[2] The abbreviations used are: ERK, extracellular signal-regulated kinase; MAP kinase, mitogen-activated protein kinase; MSK1, mitogen- and stress-activated protein kinase 1; NMDA, *N*-methyl-D-aspartate; TrkB, receptor tyrosine-kinase B; BDNF, brain-derived neurotrophic factor; CREB, cAMP-response element-binding protein; HEK-293, human embryonic kidney 293; NLS, nuclear localization signal; GFP, green fluorescent protein; MEK, MAP kinase/ERK kinase; RFP, red fluorescent protein; FRAP, fluorescence recovery after photobleaching; PBS, phosphate-buffered saline; AP, action potential; NFAT, nuclear factor of activated T cells; n/c, nuclear *versus* cytosolic; YFP, yellow fluorescent protein; PKA, protein kinase A; MBP, maltose-binding protein; AP, action potential.

sequently enters the nucleus to phosphorylate transcription factors (23).

The mechanism of ERK1/2 translocation to the nucleus is also unclear. Evidence for an active nuclear import mechanism came from experiments in which inhibitors of active import such as wheat germ agglutinin or Ran inhibitors were introduced by microinjection or digitonin-mediated permeabilization into non-neuronal cell lines such as HeLa or NIH-3T3 cells (24–26). Other experiments in HeLa cells or HEK-293 cells are consistent with ERK1/2 diffusing into the nucleus (26–28). To investigate trafficking and nuclear translocation of ERK1/2 in neurons is particularly important because of the large distances from the site of ERK1/2 activation at synapses and dendrites to the cell nucleus and the physiological relevance of this process for plasticity and learning.

We considered three possible mechanisms through which ERK1/2 can enter the nucleus. The first is passive diffusion, which requires no energy, adaptor molecules, or contact with the nuclear pore and is not blocked at low temperatures (*i.e.* 4 °C). The second mechanism is facilitated diffusion, which is energy-independent and requires contact of the protein with phenylalanine-glycine-rich protrusions in the nuclear pore. Proteins that exceed a molecular mass of about 50 kDa cannot pass the nuclear pore by passive diffusion within a time range of hours (29–31). However, proteins of this size can enter the nucleus within minutes by traversing the nuclear pore via facilitated diffusion (32). The third mechanism is the RanGDP/GTP-mediated active import, which is dependent upon the presence of a nuclear localization signal (NLS) and requires importins (33). The literature on the mechanism of ERK1/2 nuclear translocation in non-neuronal cells is controversial; diffusion processes have been proposed as well as active transport (see above), although the identification of an NLS within ERK1 or ERK2 has not been reported.

Here we investigated the dendritic trafficking and nuclear translocation of ERK1/2 in hippocampal neurons using ERK1 and ERK2 labeled with a recently developed photobleachable and photoactivable tag (34). ERK1/2 were activated either by treatment of the neurons with BDNF, which stimulates the BDNF receptor, TrkB, or by inducing action potential bursting. The latter stimulation paradigm strongly activates synaptic NMDA receptors and induces a transcription-dependent form of neuronal network plasticity akin to long term potentiation (35). The results obtained in this study show that propagation of ERK1/2 within dendrites is not signal-regulated and occurs through passive diffusion; signal-induced ERK1/2 nuclear translocation is not mediated by an active transport mechanism but by facilitated diffusion.

EXPERIMENTAL PROCEDURES

Plasmids—The following plasmids were used: ERK2-GFP and RFP-MEK1 plasmids obtained from J. S. Stork, Vollum Institute for Advanced Biomedical Research, L474, Oregon Health & Science University, Portland, OR; plasmids for ERK1-Dronpa or Dronpa obtained from A. Miyawaki, Laboratory for Cell Function and Dynamics, Advanced Technology Development Group, Brain Science Institute, Hirosawa, Japan; MEK1-Dronpa plasmid obtained from M. Matsuda, Department of Signal Transduction, Research Institute for Microbial Diseases, Osaka University, Yamadaoka, Suita-shi, Osaka, Japan.

To generate ERK2-Dronpa, cDNA encoding rat ERK2 was amplified using PCR. At the 5′ end a start codon was introduced as well as a BamHI restriction site, which was located upstream of the ATG sequence. The following primer was designed for the sense direction: 5′-ATAGGATCCTACAAGTCCGGACTCATGTCTCGAGCG-3′. At the 3′ end we removed the stop codon and generated a NotI restriction site using the following antisense primer: 5′-TCATATGCGGCCGCAAGATCTGTATCCTGGCTGGAA-3′. The resulting DNA was digested using BamHI and NotI and subcloned into a pcDNA3.1 vector containing ERK1-Dronpa replacing ERK1. To generate MBP-Dronpa, the same approach as described for ERK2-Dronpa was used. The primer sequences were 5′-CGCGTCGCGGATCCATGAAAATCGAAGAA-3′ (sense direction) and 5′-TAAGTATAGCGGCCGCGGGCTTCATCGACAGT-3′ (antisense). To generate ERK2-Dronpa-NLS, the ERK2-Dronpa construct was amplified using PCR. An NheI restriction site was generated at the 5′ end upstream of the start codon. At the 3′ end we introduced a BspEI site. The following primers were used to generate the new restriction sites: sense direction, 5′-ATATGCTAGCTACAAGTCAGGACTCATGTCTCGAGCG-3′; antisense direction, 5′-ATATTTCCGGACTTGGCCTGCCTCGGCAGCTCAGAAT-3′. The insert was subcloned into a pEYFP-Nuc vector (Clontech). Digesting the vector with NheI and BspEI removed the EYFP-Nuc gene but not the triple NLS segment. ERK2-Dronpa was ligated into the vector N-terminal of the NLS sequence.

Cell Culture and DNA Transfection—Primary hippocampal neurons from newborn Long-Evans or Sprague-Dawley rats were dissociated and plated on poly-D-lysine/laminin (BD Biosciences)-coated 12-mm coverslips or 35-mm plastic dishes (Nunc) as described by Bading and Greenberg (2) except that the growth medium was supplemented with B27 (Invitrogen). The cells were grown for 8 days in growth medium. After 3 days in culture, 2.4 μM cytosine D-arabinofuranoside (Sigma) was added to each dish to prevent proliferation of non-neuronal cells. On day 8 of *in vitro* culturing, growth medium was replaced with transfection medium, which consisted of a salt/glucose/glycine solution and minimum Eagle's medium (9:1; v/v) plus sodium selenite 10 μg/ml, insulin 15 μg/ml, transferrin 8.25 μg/ml, and penicillin-streptomycin 0.5%. Salt/glucose/glycine solution is as follows (in mM): NaCl 114, $NaHCO_3$ 26, KCl 5.3, $MgCl_2$ 1, $CaCl_2$ 2, HEPES 10, glycine 1, glucose 30, sodium pyruvate 0.5, phenol red 0.2%. DNA transfection was done on day 10 after plating using Lipofectamine 2000 (Invitrogen) at 5 μl/ml in transfection medium without penicillin-streptomycin. The total DNA concentration was 1.6 μg/μl. The Lipofectamine/DNA mixture was left on the cells for 3 h before it was replaced with transfection medium. Cells were left for an additional 36–48 h before analysis.

Confocal Imaging—All live imaging experiments were done at 37 °C unless stated otherwise. We used a confocal laser scanning microscope TCS SP2 (Leica, Mannheim, Germany) equipped with an inverted fluorescence microscope DM IRE2 (Leica) and Leica confocal scan software. In all imaging experiments gray levels were not saturated. Images represented

under "Results" were scaled to enhance contrast and artificially colored by adapting the look-up table to the color of the corresponding fluorescent tag for better representation. Coverslips containing cultured neurons were transferred into a custom-made metal chamber and mounted on the microscope stage. The chamber was filled with a CO_2-independent salt glucose glycine medium which consisted of the following (in mM): NaCl 140, KCl 5.29, $MgCl_2$ 1, $CaCl_2$ 2, HEPES 10, Glycine 1, Glucose 30, sodium pyruvate 0.5. Drugs were directly applied to the chamber. For experiments done at 37 °C, we used a heater (Life Imaging Services) to warm the air within a box (Life Imaging Services) enclosing the microscope stage. Room temperature was 22 °C. For experiments at 10 °C the perfused medium was chilled in a custom-built heat exchanger immediately before it reached the coverslip. The temperature of the medium on the coverslip was monitored. For all experiments a 40× oil immersion fluorescence objective (Leica HCX PL APO) was used. Stimulations were done either with BDNF (100 ng/ml; PeproTech) or bicuculline methiodide (50 μM; Sigma).

Imaging of ERK2-GFP—To visualize nuclear translocation of ERK2-GFP, time-lapse experiments were performed in neurons co-transfected with plasmids encoding ERK2-GFP and RFP-MEK1. Parallel scans of the RFP channel and the GFP channel were performed once per min over a time period of 45 min. Optical sections were 0.2 μm thick. Images were saved as 8-bit TIFF files with a resolution of 512 × 512 pixels, and analysis was done using ImageJ.

FRAP Experiments Using Dronpa Probes—The Dronpa signal was fully photoactivated in the whole cell using a 364 nm UV laser. The laser intensity was set to 30%, and the time of exposure was ~250 ms. A 45 × 22.5 μm area containing the soma was magnified ×8. To analyze nuclear recovery of the Dronpa probes, their fluorescence in the nucleus was fully photobleached within 3 s using the 488-nm laser line at 30% of maximal intensity. Immediately after bleaching, a 10-min time series was acquired taking one image every 30 s. The intensity of the 488 nm laser was at 1–2% of maximum to minimize bleaching of the signal.

Dendritic Trafficking of ERK1/2-Dronpa—The Dronpa signal of the whole cell was bleached to a minimum using the 488-nm laser line at 30% of maximal intensity within 10–15 s. Dendritic segments that were imaged were entirely in focus, at least 60 μm distal from the soma and spanned a distance of 90 μm. One 100-ms pulse of the 364-nm laser line at 30% of maximal power was used to reactivate the Dronpa signal in a 10-μm long area at the center of this dendritic segment. Immediately thereafter, images of Dronpa were acquired every 5 s using an excitation laser line of 488 nm at an intensity of 1–2% of maximum. The kinetics were measured at all time points by analyzing the intensities of the average Dronpa fluorescence signal at nine different regions of interest in the dendrite defined as 10-μm segments from the reactivated area.

Immunoblotting—Phosphorylation of ERK1/2, ERK2-GFP, and ERK1/2-Dronpa was measured by immunoblotting using antibodies to the phosphorylated form of ERK1/2 (rabbit polyclonal or mouse monoclonal antibody; Cell Signaling Technology, Inc.) as described previously (19, 36, 37). MBP-Dronpa was detected using a mouse monoclonal antibody against MBP (Lab Vision Corp.). Immunoblot analysis of endogenous calmodulin (monoclonal mouse-anti calmodulin antibody, Upstate Biotechnology) or tubulin (Sigma) expression was used to control for protein loading.

Immunocytochemistry—Cells were fixed with a paraformaldehyde/sucrose (4%:4%) solution. After fixation, cells were permeabilized with a methanol/acetone mixture (50:50 v/v) or with Triton X-100 (0.3%) in PBS/Tween (0.1%). Nonspecific binding sites were blocked with PBS containing 2% bovine serum albumin and 10% normal goat serum. The following primary antibodies were used: anti-phospho-ERK1/2 (rabbit, polyclonal; 1:200; Cell Signaling), anti-phospho-ERK1/2 (mouse, monoclonal; 1:200; Cell Signaling), anti-ERK1/2 (rabbit, polyclonal; 1:50; Cell Signaling), and anti-phospho-MSK1 (rabbit, polyclonal; 1:400; Cell Signaling). Fluorescein isothiocyanate-, Alexa 633-, or Cy3-conjugated goat anti-rabbit or goat anti-mouse antibodies (Jackson ImmunoResearch) were used for secondary detection. Hoechst 33258 (Serva) was used for nuclear staining.

Data Analysis—All data quoted under "Results" and plotted in graphs and histograms represent the means ± S.E. One-way analysis of variance with Tukey's post hoc test was used for all statistical analyses. All fluorescence data were background subtracted.

RESULTS

Phosphorylation and Nuclear Translocation of Endogenous ERK1/2—To activate ERK1/2, cultured rat hippocampal neurons were either treated with the neurotrophin BDNF or exposed to the γ-aminobutyric acid, type A, receptor antagonist bicuculline. Bicuculline causes the neurons to periodically fire bursts of action potentials (APs) synchronized with bursts of glutamatergic synaptic activity, which together strongly activate synaptic NMDA receptors and cause robust increases in the intracellular calcium concentration (19, 35). The induction of AP bursting was verified via electrophysiological recordings from cultured hippocampal neurons in the presence of bicuculline (supplemental Fig. 1*A*). Bursts of synaptic activity involving NMDA receptor activation are necessary for transcription-dependent hippocampal long term potentiation and memory (35, 38, 39). Similarly, the bicuculline protocol in hippocampal cultures induces a form of long lasting network plasticity that is dependent upon gene transcription, mRNA translation, and MAP kinase signaling (35). In addition, a whole genome transcriptome analysis revealed that within 2–4 h after bicuculline-induced AP bursting, several hundred genes change their expression levels (40). We first investigated whether both stimulation paradigms (*i.e.* BDNF treatment or induction of AP bursting using bicuculline) are suitable to produce physiologically relevant levels of enzymatic active endogenous phospho-ERK1/2 (pERK1/2) in the cytoplasm and, more importantly, in the nucleus. Western blot experiments using a phospho-specific ERK1/2 antibody showed that either stimulation paradigm induced phosphorylation of rat ERK1/2 at both the threonine and tyrosine residue within the conserved TEY motif, which is indicative of stimulation of ERK1/2 enzymatic activities (Fig. 1, *A* and *B*, and supplementary Fig. 2). To investigate whether these levels of pERK1/2 are sufficient to yield activated ERK1/2

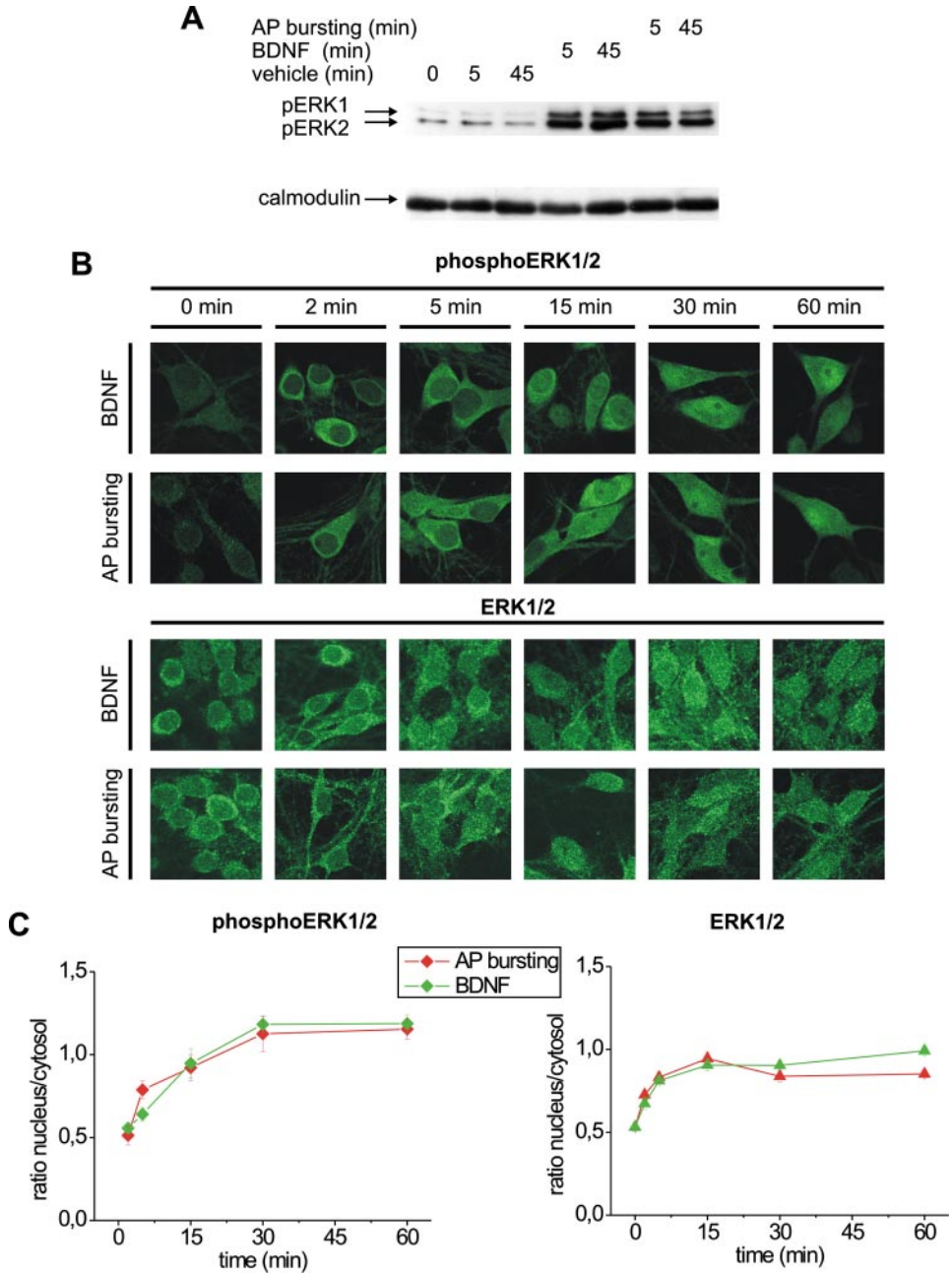

FIGURE 1. **BDNF and AP bursting induce phosphorylation and nuclear translocation of endogenous ERK1/2 in hippocampal neurons.** *A,* immunoblot analysis of ERK1/2 phosphorylation in unstimulated hippocampal neurons and in hippocampal neurons treated for 5 or 45 min with BDNF (100 ng/ml) or bicuculline (AP bursting, 50 μM), a γ-aminobutyric acid, type A, receptor antagonist that removes inhibitory synaptic activity from the neuronal network leading to action potential bursting. Calmodulin was detected as a loading control. *B* and *C,* immunocytochemical analysis of nuclear translocation of endogenous phospho-ERK1/2 and endogenous ERK1/2 in hippocampal neurons treated with BDNF (100 ng/ml) or bicuculline (AP bursting, 50 μM) for the indicated time periods. Endogenous pERK1/2 were detected immunocytochemically using a polyclonal antibody to ERK1/2 phosphorylated at the threonine and tyrosine residues within the conserved TEY motif. Endogenous ERK1/2 were detected using a polyclonal antibody directed against a conserved region of ERK1/2. Experiments were conducted in parallel preparations. Representative confocal images are shown (*B*). The nuclear/cytosolic ratio of pERK1/2 and ERK1/2 was calculated for both treatment groups at each time point (n = 11–13 for pERK1/2 and 20–30 for ERK1/2) (*C*).

in the nucleus, we analyzed MSK1, a nuclear protein kinase that is activated upon phosphorylation of Thr-581 and Ser-360. This phosphorylation event is catalyzed by ERK1/2, and the p38 MAP kinase and can be readily detected using a phospho-MSK1-specific antibody. To selectively determine the contribution of ERK1/2 to MSK1 activation, we analyzed MSK1 activation in the presence of the p38 MAP kinase inhibitor SB203580. We found that both AP bursting and BDNF treatment generated a robust phospho-MSK1 (pMSK1) signal in the absence of p38 MAP kinase activity, which is blocked in the presence of the MEK inhibitor PD98059 (supplemental Fig. 2). We next used immunocytochemistry to test whether pERK1/2 indeed signals to the nucleus. After 30 min of stimulation with either BDNF or bicuculline, a fraction of pERK1/2 appears in the nucleus. Similar to the results obtained using the Western blot analysis (see supplemental Fig. 2*A*), the appearance of the nuclear pMSK1 signal was blocked if the stimulation was done in the presence of both SB203580 and PD98059 but not in the presence of SB203580 (supplemental Fig. 2*B*). These results indicate that both the BDNF and the bicuculline stimulation paradigms used in this study are suitable to generate physiological relevant levels of endogenous nuclear pERK1/2 that are sufficient to activate MSK1, a downstream target of ERK1/2 signaling.

We next did immunocytochemical experiments to determine the localization of pERK1/2 and ERK1/2 at various times after stimulation. At early time points (*i.e.* 2 and 5 min) after stimulation ERK1/2 as well as pERK1/2 are predominantly localized to the cytoplasm. The nuclear fraction of pERK1/2 increased with time after stimulation reaching a maximum after ~30 min (Fig. 1*B*). However, a large proportion of pERK1/2 remained cytoplasmic and was distributed throughout the entire neuron, including the distal areas of the dendrites (data not shown). For both stimulation paradigms, the ratio of nuclear to cytoplasmic pERK1/2 signal (n/c ratio of average absolute 8 bit gray levels from confocal images) reached a plateau of about 1.2 at the 30- and 60-min time points (Fig. 1*C, left panel*). This indicates that pERK1/2 was slightly enriched in the nucleus following stimulation and may have surpassed concentration equilibrium. We observed that pMSK1 immunoreactivity was only slightly elevated after 2 and 5 min of stimulation and that it reached a maximum after

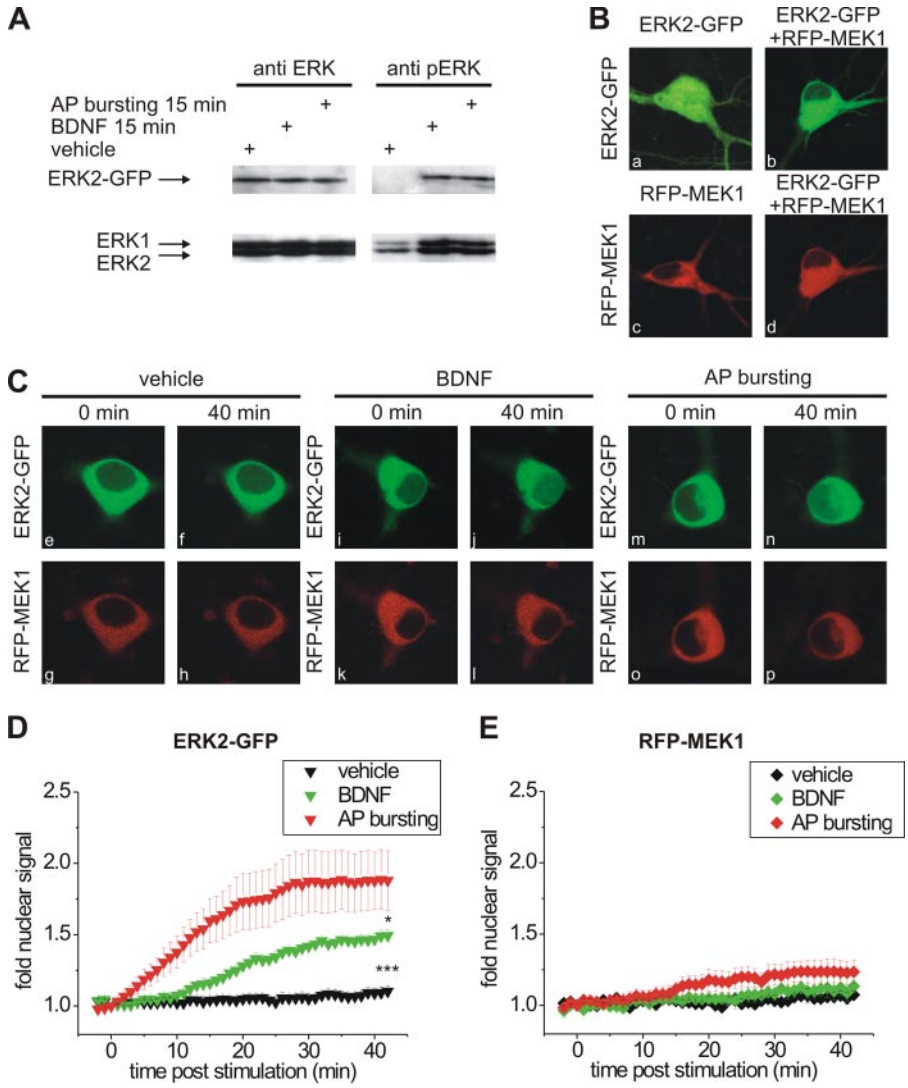

FIGURE 2. **Overexpressed GFP-ERK2 is phosphorylated and invades the nucleus during AP bursting or BDNF treatment and its cytoplasmic retention in untreated neurons requires co-expression of RFP-MEK1.** *A,* immunoblot analysis of ERK2-GFP expression and its phosphorylation in ERK2-GFP/RFP-MEK1 co-transfected hippocampal neurons left untreated or treated for 15 min with BDNF (100 ng/ml) or bicuculline (AP bursting, 50 μM). Endogenous ERK1/2 or pERK1/2 was detected as well and serves as a loading/stimulation control. *B,* confocal imaging of ERK2-GFP and RFP-MEK1 overexpressed in hippocampal neurons either single-transfected with cDNA encoding ERK2-GFP (*panel a*) or RFP-MEK1 (*panel c*) or co-transfected with both constructs (*panels b* and *d*). *C,* confocal imaging of ERK2-GFP and RFP-MEK1 in co-transfected hippocampal neurons left either unstimulated (*vehicle*) or treated with BDNF (100 ng/ml) or bicuculline (AP bursting, 50 μM). Representative images of the ERK2-GFP or RFP-MEK1 distribution are shown for a time points prior to stimulation (0 min) and after 40 min of stimulation. *D* and *E,* analysis of nuclear localization of ERK2-GFP (*D*) and RFP-MEK1 (*E*) in the presence of BDNF ($n = 5$), during AP bursting ($n = 8$) or in vehicle-treated cells ($n = 5$). Neurons were co-expressing ERK2-GFP and RFP-MEK1. The fold increase of the initial nuclear fluorescence levels was calculated from confocal images acquired over a time period of 45 min. Drugs were applied at $t = 0$. Statistically significant differences are indicated with *asterisks*. (* = $p < 0.05$; *** = $p < 0.001$.)

30 min of either AP bursting or BDNF stimulation (data not shown). The kinetics of MSK1 phosphorylation match those of nuclear enrichment of pERK1/2.

In contrast to pERK, the n/c ratio of ERK1/2 did not exceed 1 after stimulus-induced nuclear translocation (Fig. 1*C, right panel*). The difference in the n/c ratios of pERK and ERK may be due to the presence of dephosphorylated ERK1/2 in the cytoplasm but not the nucleus. This fraction of dephosphorylated ERK1/2 is not seen in the pERK1/2 staining and contributes to the ERK1/2 n/c ratio but not the pERK1/2 n/c ratio. In addition, the kinetics of the changes of the ERK1/2 n/c ratio appear faster than that of pERK1/2 possibly because pERK appears in the cytosol before it enters the nucleus reducing the n/c ratio at earlier time points. Alternatively, the differences in the n/c ratios may be due to differences in the rates of de-phosphorylation of pERK in the nucleus and the cytoplasm; if pERK is dephosphorylated faster in the cytoplasm than in the nucleus, the n/c ratio for pERK is expected to exceed 1. It is also conceivable that n/c ratios marginally in excess of 1 may simply be due to the properties of small exogenous fluorescent proteins that produce a brighter nuclear than cytosolic signal because of fewer organelles per unit volume in the nucleus (41). Clearly, the localization of ERK and pERK1/2 differs significantly from that of proteins containing a nuclear localization signal (NLS) such as nuclear factor κB or NFAT. Active transport of such proteins causes them to localize virtually exclusively to the nucleus (42, 43).

Live Imaging of ERK1/2 Trafficking—By adapting an approach used previously in COS-7 cells (34), we began live imaging of ERK1/2 trafficking in neurons using GFP-tagged ERK2 (ERK2-GFP). An expression vector for ERK2-GFP was transfected together with an expression vector for RFP-tagged MEK1 (RFP-MEK1) into cultured hippocampal neurons. Western blot experiments demonstrate that similar to the endogenous ERK1/2, ERK2-GFP co-expressed with RFP-MEK1 was phosphorylated upon BDNF stimulation or induction of AP bursting (Fig. 2*A*). The localization of ERK2-GFP in unstimulated hippocampal neurons depends on the presence of RFP-MEK1. In the absence of RFP-MEK1, ERK2-GFP was evenly distributed throughout the nucleus and cytoplasm (n/c ratio, 1.08 $\pm$ 0.06) (Fig. 2*B*). Stimulation of the neurons either with BDNF or by inducing AP bursting for up to 45 min did not change the distribution pattern (data not shown). In the presence of RFP-MEK1, ERK2-GFP was localized predominantly to the cytoplasm of unstimulated neurons (n/c = 0.43 $\pm$ 0.03) (Fig. 2*B*). This was also observed in cells weakly expressing ERK2-GFP and not co-expressing RFP-MEK1 (data not shown). These differences in the localization of ERK2-GFP are because of the one-to-one stoichiometry of the

ERK2-GFP interaction with RFP-MEK1. MEK1 contains a nuclear export signal (44, 45) resulting in the cytoplasmic localization of RFP-MEK1 and the ERK2-GFP·RFP-MEK1 complex (Fig. 2*B*). In contrast, ERK2-GFP not in complex with RFP-MEK1 is not actively exported from the nucleus. Note that the n/c ratio of ERK2-GFP in presence of RFP-MEK1 is in the range of endogenous ERK1/2 (0.43 ± 0.03 *versus* 0.53 ± 0.02).

We next determined the kinetics of the increase in nuclear ERK2-GFP signal upon the stimulus-induced phosphorylation of ERK2-GFP that triggers the release of ERK2-GFP from its complex with RFP-MEK1 (46). ERK2-GFP and RFP-MEK1 signals were imaged over a time course of 45 min following BDNF treatment or induction of AP bursting. During this period the nuclear signal of ERK2-GFP rose markedly, whereas no change in the nuclear RFP-MEK1 signal was observed (Fig. 2*C*). BDNF-induced nuclear influx of ERK2-GFP was detectable after ~10 min of stimulation (Fig. 2*D*). In the case of AP bursting, ERK2-GFP nuclear translocation started virtually immediately after the stimulation and proceeded at a slightly faster rate than was seen following BDNF treatment to reach a plateau after about 25 min. Neither stimulation paradigm affected the subcellular distribution of RFP-MEK1 (Fig. 2*E*).

Distinct Properties of Several Dronpa Fusion Proteins—To investigate the mechanism by which ERK1/2 translocates to the nucleus, we wished to compare the kinetics of nuclear translocation of ERK1/2 with that of comparable molecules that diffuse freely or undergo active transport into the nucleus. We generated several fusion proteins containing a photoactivable tag and quantified their movement in live neurons. This was achieved by fusing our proteins of interest to Dronpa, a Pectinidae coral-derived fluorescent protein with reversible photoswitching properties. Dronpa is photobleached by excitation at 490 nm, but its fluorescence can be restored with 400-nm irradiation (34). In contrast to conventional GFP variants, Dronpa is rapidly photobleached with minimal light intensity (and thus much less photodamage and nonspecific effects) and can be reactivated and rebleached repeatedly, making it an excellent flexible tool for fluorescence recovery after photobleaching (FRAP) experiments. We tested Dronpa and ERK1-Dronpa (34) as well as the following three additional Dronpa fusion proteins that we generated: ERK2-Dronpa, ERK2-Dronpa-NLS, and MBP-Dronpa.

To investigate whether overexpression of Dronpa fusion proteins compromises the electrical properties of neurons, we measured resting membrane potential, series resistance, and the ability of bicuculline to induce AP bursting in MBP-Dronpa- or ERK1-Dronpa-transfected hippocampal neurons. We found that neurons overexpressing these proteins did not differ in these properties from untransfected neurons (data not shown).

ERK2-Dronpa-NLS contains at the C terminus three copies of an NLS. The fusion of NLS to ERK2-Dronpa is unlikely to compromise its binding to MEK1, because the interaction between MEK1 and ERK2 occurs at the central docking domain of ERK2 (47) and insertion of fluorescent tags at the N terminus or C terminus are compatible with ERK2 binding to MEK1 (48). The ERK2-Dronpa-NLS fusion protein localized exclusively to the nucleus regardless of whether it was expressed alone or co-expressed with RFP-MEK1 (Fig. 3) or whether cells were stimulated with either BDNF or by induction of AP bursting (data not shown). The constitutive nuclear localization of ERK2-Dronpa-NLS precluded an analysis of nucleo-cytoplasmic shuttling using FRAP.

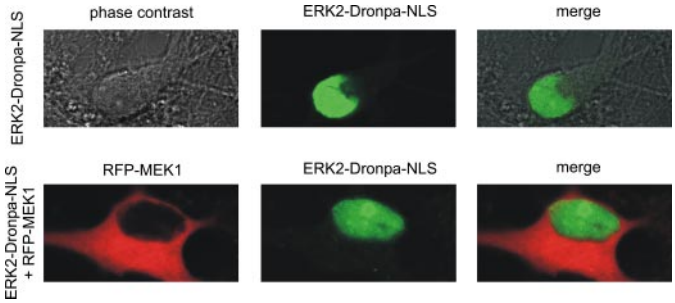

FIGURE 3. **ERK2-Dronpa-NLS is entirely localized to the nucleus, even in the presence of RFP-MEK1.** *Upper row,* hippocampal neurons were transfected with ERK2-Dronpa-NLS. A phase contrast, a confocal fluorescence image, and a merge of the two images of the same cell are depicted. The *lower row* represents a hippocampal neuron co-transfected with RFP-MEK1 and ERK2-Dronpa-NLS. Note the exclusive localization of ERK2-Dronpa to the nucleus in both single- and co-transfected cells.

MBP is a bacterial protein with a globular tertiary structure, which does not associate with MEK and is believed to freely diffuse in mammalian cells and undergo neither active nuclear import nor nuclear export (49, 50). The size of MBP-Dronpa (~67 kDa) is comparable with that of ERK1-Dronpa, ERK2-Dronpa (collectively referred to as ERK1/2-Dronpa) (71/69 kDa), and ERK2-Dronpa-NLS (72 kDa) (ERK1/ERK2 alone are 44/42 kDa), all of which exceed the 40–50-kDa size limit for unrestricted passive diffusion through the nuclear pore complex (30, 51). Molecules larger than 40–50 kDa can, however, also diffuse into the nucleus but at a much slower speed (33). Dronpa alone has a molecular mass of 27 kDa and is assumed to freely diffuse into and out of the nucleus.

In contrast to ERK2-Dronpa-NLS, Dronpa, ERK1-Dronpa, ERK2-Dronpa, and MBP-Dronpa were localized both to the cytoplasm and the nucleus in cells transfected with each respective construct (Fig. 4, *A* and *B, pre-bleach*). The n/c ratios of the latter four proteins were similar (Dronpa, 1.37 ± 0.17; ERK1-Dronpa, 1.19 ± 0.17; ERK2-Dronpa, 1.42 ± 0.10; MBP-Dronpa, 1.16 ± 0.07; Fig. 4*B*, *left panel, pre-bleach*) and markedly different ($p < 0.001$) from that of ERK2-Dronpa-NLS (transfected alone, 7.87 ± 1.29; co-transfected with MEK1-RFP, 9.14 ± 2.09) The nuclear translocation properties of ERK1/2-Dronpa resembled those of freely diffusing molecules, Dronpa and MBP-Dronpa, and differ strikingly from those of the actively imported proteins ERK2-Dronpa-NLS. Although this points to a diffusion process underlying the entry of ERK1/2 into the nucleus, it does not distinguish between passive and facilitated diffusion.

Nuclear Shuttling of Photoactivable Forms of ERK1/2—FRAP experiments revealed a continuous shuttling of ERK1/2-Dronpa across the nuclear border in the absence of RFP-MEK1. Following bleaching of the nuclear Dronpa signal, we measured the recovery of nuclear fluorescence in 30-s intervals over a period of 10 min. This revealed different rates of FRAP for the different proteins (Fig. 4, *A–C*). The recovery rates of the nuclear signal for ERK1-Dronpa and ERK2-Dronpa were not

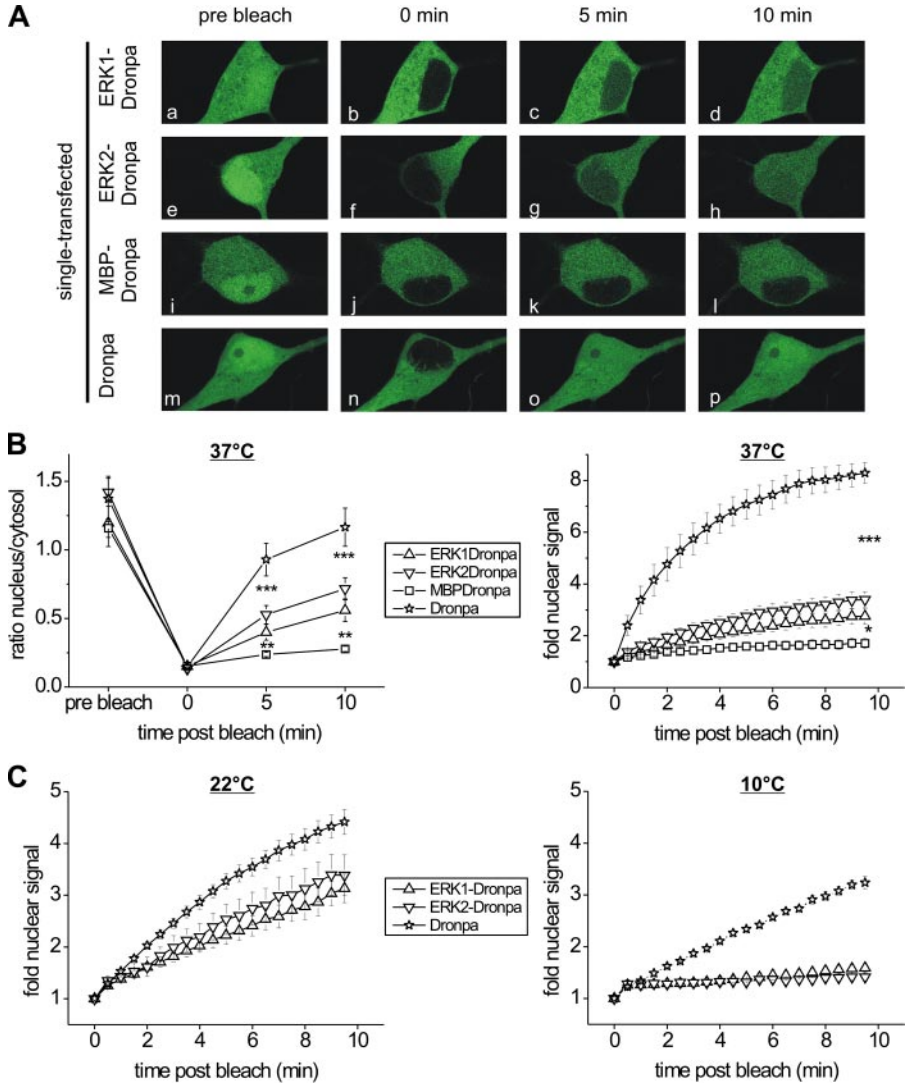

FIGURE 4. **Nuclear translocation of ERK1/2-Dronpa occurs at faster rates than MBP-Dronpa and is temperature-sensitive.** *A,* FRAP analysis of steady-state nuclear turnover rates of ERK1-Dronpa, ERK2-Dronpa, MBP-Dronpa, or Dronpa in neurons expressing these proteins in the absence of RFP-MEK1. Representative confocal images show the Dronpa signal in the same neuron before the FRAP experiment (*pre-bleach*), immediately (*0 min*), and 5 and 10 min after photobleaching of Dronpa. *B,* kinetic analysis of the experiment depicted in *A* for ERK1-Dronpa ($n = 8$), ERK2-Dronpa ($n = 10$), MBP-Dronpa ($n = 8$), and Dronpa ($n = 11$). The ratio between nuclear and cytosolic Dronpa fluorescence is plotted in the *left panel* for the same time points as in *A*. The fold increase of nuclear fluorescence immediately after bleaching is plotted in the *right panel* over a time period of 10 min. Nuclear signals are normalized to nuclear fluorescence levels immediately after bleaching. (* = $p < 0.05$; ** = $p < 0.01$; *** = $p < 0.001$.) *C,* nuclear translocation of ERK1/2-Dronpa is blocked at 10 °C. FRAP experiments were performed in single-transfected, unstimulated neurons at the temperatures indicated. ($n = 5$ for all groups.)

different from each other but were much slower than that of Dronpa and faster than that of MBP-Dronpa (Fig. 4*C*, for *panels n* and *p* values see figure legend). The rate of FRAP for all Dronpa fusion proteins tested was independent of the stimulation of the neurons either with BDNF or by inducing AP bursting in the absence of overexpressed MEK1 (data not shown). These FRAP results suggest that ERK1-Dronpa and ERK2-Dronpa do not enter the nucleus as fast as would be expected for passive diffusion of a freely diffusing molecule such as Dronpa, but faster than would be expected for unassisted entry of an ~70-kDa molecule such as MBP-Dronpa. Some process thus appears to weakly assist the entry of ERK1/2 into the nucleus.

Temperature Sensitivity of ERK1/2-Dronpa Nuclear Translocation—Unlike passive diffusion that decreases in a linear fashion with decreasing temperature, facilitated diffusion decreases in a nonlinear way with decreasing temperature and is nearly abolished at 4 °C (29, 32). We therefore measured nuclear translocation of ERK1/2-Dronpa and Dronpa at 37, 22, and 10 °C (Fig. 4, *B* and *C*). The nuclear translocation of Dronpa showed a virtually linear decrease in speed as the temperature dropped from 37 to 22 °C and to 10 °C. In contrast, the recovery of the nuclear ERK1/2-Dronpa signals appeared unaffected by the drop from 37 to 22 °C but was almost abolished at 10 °C indicating a nonlinear temperature dependence. This characteristic temperature dependence suggests that ERK1/2-Dronpa diffusion into the nucleus involves assisted nuclear translocation (*i.e.* facilitated diffusion or active import) rather than passive diffusion.

Kinetics of Stimulation-induced Nuclear Translocation of ERK1/2-Dronpa—We next investigated the kinetics of signal-induced ERK1/2-Dronpa translocation. For this we selected neurons expressing ERK1/2-Dronpa at very low levels. It was shown in NIH-3T3 cells that recombinant ERK1/2 expressed at low levels do not saturate endogenous mechanisms that are responsible for their physiological subcellular localization (24). We found that in neurons expressing low levels of ERK1-Dronpa, ERK1/2 immunoreactivity was only 1.89-fold (±0.12) stronger than that of untransfected cells; in contrast, in neurons expressing high levels of ERK1-Dronpa, ERK1/2 immunoreactivity was 5.8-fold (±0.49) stronger than that of untransfected cells (supplemental Fig. 3, *A* and *B*). In the "low expression" cells, the n/c ratio of ERK1/2-Dronpa was similar to that of endogenous ERK1/2 (ERK1-Dronpa, 0.56 ± 0.03; ERK2-Dronpa, 0.66 ± 0.04; endoERK1/2, 0.53 ± 0.03) under basal conditions. This indicates that the endogenous mechanisms responsible for excluding ERK from the nucleus were not saturated in these low expression cells. Upon stimulation with BDNF or following induction of AP bursting, ERK1/2-Dronpa translocated to the nucleus reaching n/c ratios of ~1 (ERK1-Dronpa, 1.07 ± 0.12 AP bursting; 1.21 ± 0.13 BDNF and ERK2-Dronpa, 0.82 ± 0.05 AP bursting; 1.06 ± 0.08 BDNF; supple-

mental Fig. 3, *C* and *D*, and data not shown). FRAP experiments revealed a significantly faster recovery of the nuclear ERK1/2-Dronpa signal after stimulation than after vehicle treatment (supplemental Fig. 3, *C* and *D*). Because of the low expression levels of the Dronpa fusion proteins, the signal-to-noise ratio was compromised, and the variability of the results increased. It was not possible to solve this problem by using stronger laser intensities because of the photoconversion properties of Dronpa.

We next co-expressed RFP-MEK1 together with ERK1-Dronpa or ERK2-Dronpa; this yielded, under basal conditions, a nearly exclusively cytoplasmic localization of ERK1/2-Dronpa that was largely independent of the expression levels of the Dronpa fusion proteins. Expression of RFP-MEK1 did not change the localization of MBP-Dronpa (compare Fig. 5*A*, *panel m*, with Fig. 4*A*, *panel i*) or that of Dronpa (data not shown). Upon stimulation with BDNF or following induction of AP bursting, ERK2-Dronpa translocated to the nucleus (Fig. 5*A*, *panels e* and *i*). Western blot experiments using pERK1/2-specific antibodies demonstrate that either stimulation paradigm increased the phospho-ERK1-Dronpa and phospho-ERK2-Dronpa signal by a factor similar to that observed with the endogenous ERK1/2 proteins (supplemental Fig. 4). Immunocytochemical assessment of pERK1/2 levels in individual cells revealed that 15 min after BDNF stimulation, pERK1/2 immunoreactivity in neurons expressing RFP-MEK1 and ERK2-Dronpa was more than twice of that detected in untransfected neurons (supplemental Fig. 4*A*); average absolute 8-bit gray levels were 129 ± 17 in transfected cells and 61 ± 5 in untransfected cells.

Similar to the neurons expressing ERK1-Dronpa and ERK2-Dronpa at low levels, the n/c ratios for ERK1/2-Dronpa in cells co-expressing RFP-MEK1 increased following AP bursting or BDNF stimulation (Fig. 5*A, panels e* and *i*). FRAP experiments performed between 10 and 30 min after onset of the stimulation revealed a significantly faster rate of nuclear translocation of ERK1/2-Dronpa in neurons stimulated with either BDNF or AP bursting than in vehicle-treated neurons (Fig. 5). The increases in nuclear ERK1-Dronpa signal 10 min after bleaching were 1.39 ± 0.07-fold (unstimulated, $n = 8$), 2.50 ± 0.14-fold (BDNF, $n = 9$), and 2.76 ± 0.23-fold (AP bursting, $n = 9$). The increases in nuclear ERK2-Dronpa signal 10 min after bleaching were 1.44 ± 0.16-fold (unstimulated, $n = 5$), 2.58 ± 0.17-fold (BDNF, $n = 6$), and 2.13 ± 0.13-fold (AP bursting, $n = 10$). Compared with unstimulated cells, the recovery of nuclear ERK1/2-Dronpa was significantly larger in BDNF-treated and AP-bursting cells ($p < 0.001$ in all cases).

The subcellular distribution of MBP-Dronpa was not altered by RFP-MEK1 co-expression and appeared not to be different from the localization of ERK1/2-Dronpa after stimulation. Similar to the result obtained with hippocampal neurons expressing only MBP-Dronpa (see Fig. 4*B*), in neurons expressing both MBP-Dronpa and RFP-MEK1, the MBP-Dronpa nuclear signal recovered to a lesser degree and at a slower rate than those of ERK1/2-Dronpa (Fig. 5). Neither AP busting nor BDNF treatment altered the nuclear recovery rate of MBP-Dronpa. The increases in nuclear MBP-Dronpa signal during a 10-min post-bleach period were 1.51-fold ± 0.13 (unstimulated, $n = 8$), 1.32-fold ± 0.09 (BDNF stimulation, $n = 5$), and 1.46-fold ± 0.12 (AP bursting, $n = 5$).

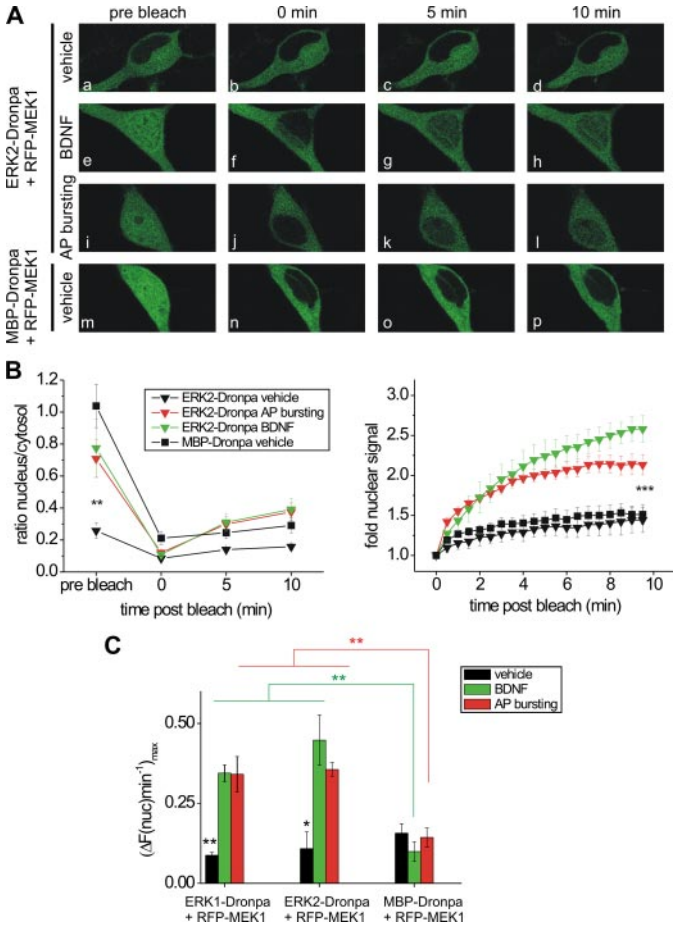

FIGURE 5. **Facilitated diffusion of highly expressed ERK1/2-Dronpa across the nuclear envelope is dependent on stimulation in the presence of RFP-MEK1.** *A,* FRAP analysis of stimulation-induced nuclear turnover rates of ERK2-Dronpa. Hippocampal neurons were co-transfected with RFP-MEK1 and either ERK2-Dronpa or MBP-Dronpa and stimulated as indicated. Representative images show the Dronpa signal in the same neuron before the FRAP experiment (*pre-bleach*), immediately (*0 min*), and 5 and 10 min after photobleaching of Dronpa. FRAP experiments were performed between 10 and 30 min from the onset of stimulation. *B,* kinetic analysis of the experiment depicted in *A*. The ratio between nuclear and cytosolic Dronpa fluorescence is plotted in the *left panel* for the same time points as in *A*. The fold increase of nuclear fluorescence of ERK2-Dronpa or MBP-Dronpa during 10 min after bleaching is plotted in the *right panel*. Nuclear signals are normalized to nuclear fluorescence levels immediately after bleaching. *C,* maximal slopes of nuclear FRAP of ERK1-Dronpa, ERK2-Dronpa, and MBP-Dronpa are plotted for hippocampal neurons co-transfected with RFP-MEK1 and stimulated as indicated. The maximal fold increase per min of the nuclear fluorescence signal indicates the maximal influx rate of the Dronpa-tagged proteins. See "Results" for cell numbers. (* = $p < 0.05$; ** = $p < 0.01$; *** = $p < 0.001$.)

As an additional parameter that characterizes the kinetics of nuclear translocation, we measured the maximal rate of increase of nuclear fluorescence (Figs. 5*C* and 6*C*). The nuclear influx of ERK1-Dronpa and ERK2-Dronpa was stimulation-dependent and faster than that of MBP-Dronpa (Fig. 5, *B* and *C*). The values for maximal rate of change in nuclear fluorescence for ERK1-Dronpa and ERK2-Dronpa during stimulation were significantly larger than those of MBP-Dronpa ($p < 0.01$; Fig. 5*C*). The measurements obtained for MBP-Dronpa reflect the kinetics of passive diffusion into the nucleus of a 67-kDa protein. ERK1/2-Dronpa are similar in size to MBP-Dronpa but

exhibited much faster nuclear translocation rates, indicating that movement of ERK1/2-Dronpa into the nucleus involves facilitated rather than passive diffusion.

To confirm that nuclear translocation and AP bursting occur in the same cell during bicuculline stimulation, we made simultaneous electrophysiological and live imaging recordings from individual neurons overexpressing RFP-MEK1 and ERK1-Dronpa. Imaging of ERK1-Dronpa over 45 min in the presence of bicuculline revealed that synchronized AP bursting and ERK1-Dronpa nuclear translocation are coupled (supplemental Fig. 1, *B* and *C*).

There is evidence that activation of protein kinase A (PKA) is crucial for ERK-dependent transcription of genes that are regulated by CREB (52). Because it was not clear if either of the stimulation paradigms employed in this study were able to activate PKA in sufficient quantities, we selectively induced PKA activity with forskolin. If nuclear translocation of ERK1/2 follows a different mechanism downstream of PKA, this should be revealed in the kinetics of ERK1/2-Dronpa FRAP. We found that ERK1/2 as well as ERK1-Dronpa were phosphorylated to the same extent during forskolin stimulation and BDNF stimulation or AP bursting (supplemental Fig. 5*A*). Also nuclear shuttling of ERK1-Dronpa was identical during all three modes of stimulation (supplemental Fig. 5*B*).

Signal-induced Nuclear Shuttling of ERK1/2-Dronpa Is Blocked at Low Temperatures—We next repeated the FRAP experiments at 22 and 10 °C. To yield comparable levels of ERK1/2 activation, stimulation was done at 37 °C for 30 min before the temperature was quickly lowered to the desired value. The n/c ratio of ERK1-Dronpa was close to one in all cases indicating that the ERK pathway had been successfully activated (BDNF, 0.90 ± 0.11 at 10 °C, 0.87 ± 0.09 at 22 °C, and 1.06 ± 0.12 at 37 °C; AP bursting, 0.92 ± 0.09 at 10 °C, 1.16 ± 0.17 at 22 °C, and 0.86 ± 0.08 at 37 °C; see Fig. 6*A*). This stimulation-induced nucleo-cytoplasmic shuttling was not altered at 22 °C but almost completely blocked at 10 °C (Fig. 6*A*). These findings are similar to those obtained in unstimulated hippocampal neurons transfected with ERK1- or ERK2-Dronpa (see Fig. 4); they indicate that ERK1/2-Dronpa activated via AP bursting or BDNF enter the nucleus by an assisted mechanism (*i.e.* facilitated diffusion or active transport).

Nuclear Influx of ERK1/2-Dronpa Is Independent of a Nucleo-cytoplasmic Concentration Gradient—To investigate whether the rates of nuclear influx of ERK1/2-Dronpa is dependent on a nucleo-cytoplasmic concentration gradient of ERK1/2-Dronpa, we compared nuclear influx at time points immediately after the stimulation where n/c ratios were much less than 1, and phosphorylation levels of ERK1/2-Dronpa were already maximal and at later time points after the stimulation where the concentration gradient for ERK1/2-Dronpa no longer existed (*i.e.* n/c ratio ~1). Multiple FRAP experiments were done on the same cells at time points 2, 20, and 40 min after BDNF stimulation with full photoreactivation being performed before commencing successive FRAP experiments (Fig. 6*B*). A concentration gradient was still present 2 min after BDNF stimulation but not at 20 or 40 min after stimulation (Fig. 6*B, left, pre-bleach*). The time course (Fig. 6*B*, *right*) and maximum rate (Fig. 6*C*) of changes in the nuclear signal of ERK1-Dronpa

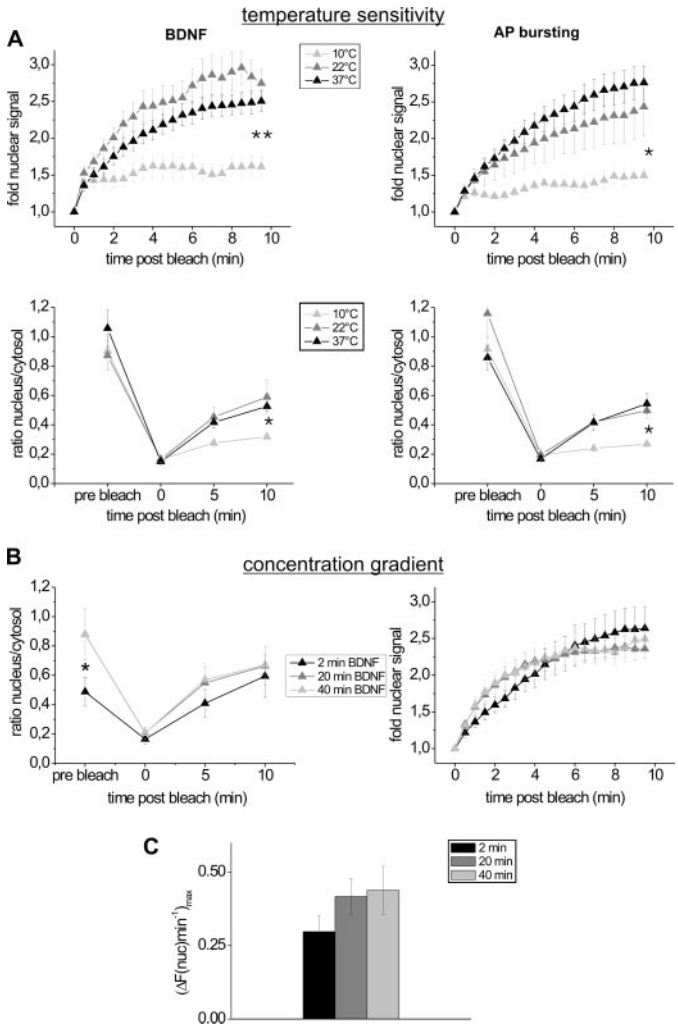

FIGURE 6. **Stimulation-induced nuclear translocation of ERK1-Dronpa is sensitive to low temperatures.** *A,* FRAP experiments were done as described previously. To analyze nuclear translocation of ERK1-Dronpa at temperatures lower than 37 °C, the MAP kinase cascade was activated for 30 min at 37 °C using either BDNF or bicuculline to induce AP bursting. The temperature was subsequently reduced to 22 or 10 °C before commencing FRAP experiments in exactly the same fashion as described for Fig. 5. *B,* influx of ERK1/2-Dronpa into the nucleus occurs continuously even in the absence of a concentration gradient. FRAP experiments were done at $t = 2$ min, $t = 20$ min, and $t = 40$ min of BDNF stimulation (100 ng/ml) in the same neurons transfected with ERK1-Dronpa and RFP-MEK1 ($n = 6$). An ERK1-Dronpa gradient between cytoplasm and nucleus is apparent after 2 min but not after 20 or 40 min of stimulation (see nucleus/cytosol ratio pre-bleach, *left panel*). Data are plotted as indicated in Fig. 5*B*. *C,* maximal nuclear influx rate of ERK1-Dronpa was measured at 2, 20, and 40 min of BDNF stimulation. Analysis was done in the same way as in Fig. 5*C*. (* = $p < 0.05$; ** = $p < 0.01$.)

showed a trend toward faster nuclear influx after 20 and 40 min of stimulation; however, this difference did not reach significance. Similar results were also obtained for ERK2-Dronpa and for the stimulation paradigm, AP bursting (data not shown). This indicates that the presence of a concentration gradient (*i.e.* at the 2-min time point) does not increase the speed of nuclear translocation of ERK1/2-Dronpa.

Diffusion Underlies Dendritic Movement of ERK1/2-Dronpa—We next analyzed ERK1/2-Dronpa trafficking in dendrites. The Dronpa signal in the entire cell was photobleached, before the fluorescence signal was photoactivated in a 10-μm diameter circular region of a straight segment of the dendrite at least 90

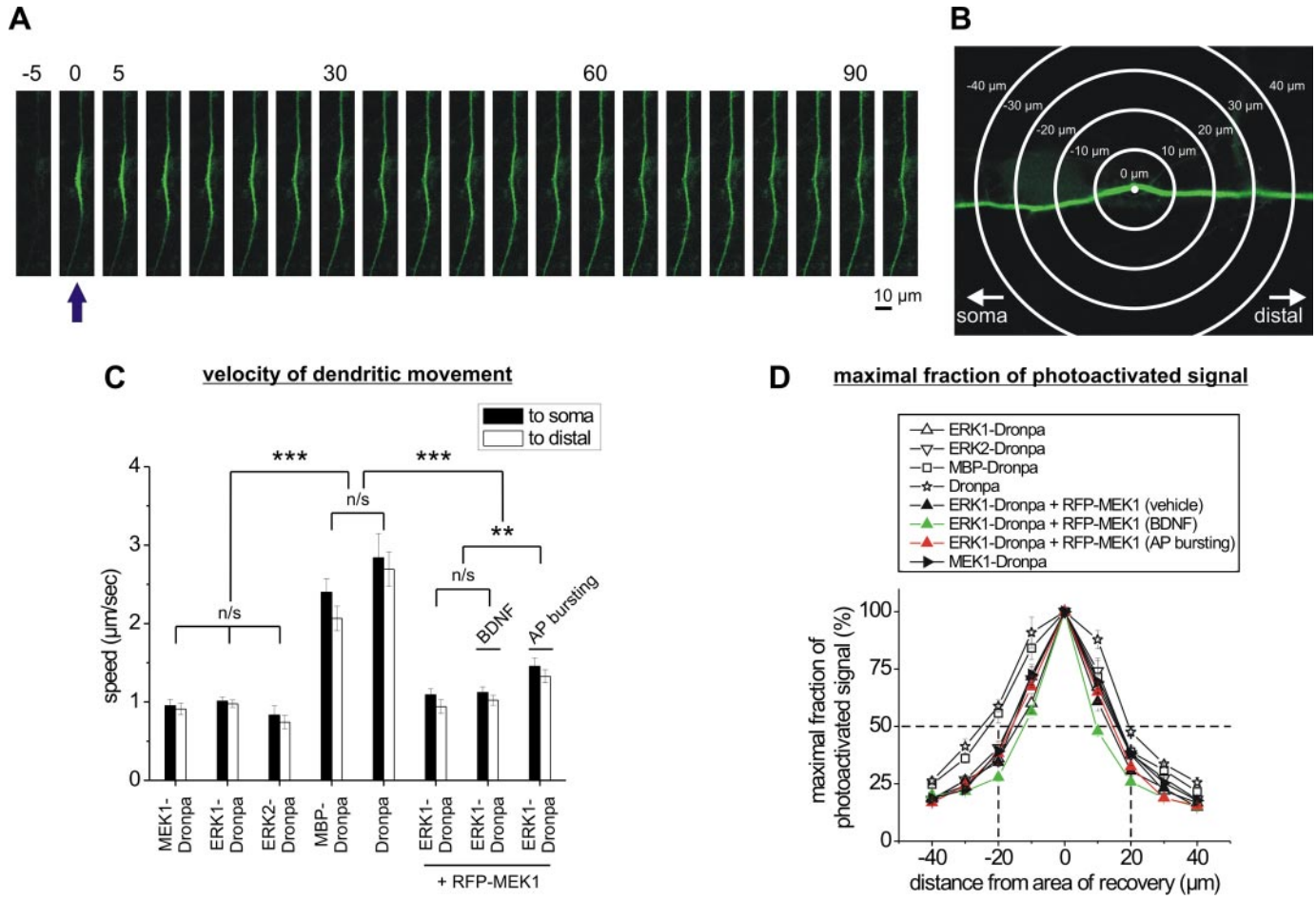

FIGURE 7. **Dendritic trafficking of ERK1/2-Dronpa is not directional and their kinetics is only slightly affected by stimulation.** *A,* representative images showing dissipation of the Dronpa signal in dendrites of cultured hippocampal neurons co-transfected with ERK1-Dronpa and RFP-MEK1. The Dronpa signal was photobleached in the whole neuron (−5 s) and reactivated locally in a dendrite (0 s; see *arrow*). The signal was then imaged every 5 s. *Numbers above* the images indicate time in seconds after reactivation. *B,* Dronpa fluorescence was measured in 9 regions of interest at the indicated distances from the region of activation every 5 s for 1.5 min. *C,* analysis of dendritic trafficking of MEK1-Dronpa, ERK1/2-Dronpa, MBP-Dronpa, and Dronpa. Hippocampal neurons were transfected as indicated *below the graph*. ERK1-Dronpa/RFP-MEK1 co-transfected neurons were treated with BDNF (100 ng/ml) or bicuculline (AP-bursting, 50 μM) or were left unstimulated as control (vehicle). The velocities of the different overexpressed proteins were measured and are plotted. (** = $p < 0.01$; *** = $p < 0.001$, $n = 6–12$.) *D,* analysis of the dissipation of MEK1-Dronpa, ERK1/2-Dronpa, MBP-Dronpa, and Dronpa in neuronal dendrites. The maximal fraction across the entire time course of stimulation of overexpressed, photoreactivated proteins that reached the nine regions of interest depicted in *B* is plotted for the same groups as shown in *C*. The *dashed horizontal line* indicates where the signal was half-maximal. The *vertical lines* refer to the Dronpa-signals 20 μm distal from the area of reactivation.

μm long (Fig. 7*A*). The dissipation of the signal was monitored over time in both directions from the area of reactivation (Fig. 7*B*). We measured the time required for the maximum of the photoactivated fluorescence signal to appear at different distances from the area of photoactivation.

In cells transfected with a single construct (encoding either Dronpa, MBP-Dronpa, MEK1-Dronpa, ERK1-Dronpa, or ERK2-Dronpa), we found that the respective proteins were moving in both directions at equal speeds. Dronpa and MBP-Dronpa were diffusing at comparable speeds throughout the dendrite despite their different sizes. Compared with Dronpa and MBP-Dronpa, ERK1/2-Dronpa moved at significantly slower speeds, which may be due to these proteins interacting with other molecules in the cell (Fig. 7*C*). The rate of ERK1-Dronpa movement in the dendrites was largely unaffected by co-expression of RFP-MEK1. In neurons co-transfected with RFP-MEK1 and ERK1-Dronpa, a small but significant increase in the diffusion kinetics for ERK1-Dronpa was observed after induction of AP bursting but not after stimulation with BDNF (Fig. 7*C*). MEK1-Dronpa moved at a speed similar to that of ERK1-Dronpa expressed either alone or co-expressed with RFP-MEK1 in unstimulated neurons (see Fig. 7*C*).

We finally investigated the range of ERK1-Dronpa-mediated signal spreading in dendrites and measured the maximal signal strength of ERK1/2-Dronpa, MEK1-Dronpa, MBP-Dronpa, and Dronpa at different distances from the area of photoreactivation across the entire time course of stimulation. We found that all proteins tested have a comparable reach. In each case, the signal dissipated equally in both directions, which was largely independent of co-expression of RFP-MEK1 or stimulation of the neurons either with BDNF or by inducing AP bursting (Fig. 7*D*). Within a distance of about 20 μm, the photoreactivated ERK1- and ERK2-Dronpa signal had dropped below 50%, illustrating the limited range of action of ERK1/2-Dronpa.

DISCUSSION

In this study we used GFP-ERK2 and photoactivable forms for ERK1 and ERK2 to analyze, in real time, dendritic trafficking and nuclear translocation of ERK1/2 in hippocampal neurons. The results indicate that synapse/dendrite-to-nucleus signaling by ERK1/2 is mediated by passive and facilitated diffusion. Given the limited reach and slow diffusion speeds of ERK1/2, their activation at synapses located at distances of more than 100 μm from the soma is unlikely to give rise to a robust nuclear translocation of activated ERK1/2 and thus may fail to couple to transcriptional regulation.

The Dynamics of Localization of ERK1/2 Not Complexed with MEK1—Similar to what has been described for cell lines (27, 46), we found that in unstimulated hippocampal neurons co-expression of MEK1 is required to restrict the localization of ERK1/2-Dronpa and ERK2-GFP to the cytoplasm when the ERK fusion proteins are overexpressed in large quantities. In the absence of exogenously expressed MEK1, ERK1/2-Dronpa and ERK2-GFP localized to both the cytoplasm and the nucleus, a distribution pattern similar to the passively diffusing proteins Dronpa and MBP-Dronpa. The addition of an NLS to ERK2-Dronpa resulted in an exclusive nuclear localization of the fusion protein even when overexpressed in high quantities. The vast differences in the nuclear translocation of ERK1/2-NLS and ERK1/2 indicate that a strong, classical NLS is unlikely to mediate nuclear translocation of the latter. It remains possible that upon phosphorylation, ERK1/2 reveal a weak NLS that assists their transport to the nucleus or that activated ERK1/2 transiently interact with other proteins in the cytoplasm that are actively transported to the nucleus via a weak NLS (53). Thus, although a strong NLS-mediated import is not mediating ERK1/2 nuclear translocation, we cannot fully exclude the possibility that active import also contributes to nuclear translocation of ERK1/2 via a weak NLS.

A careful consideration of size, speed, and temperature dependence allowed us to distinguish between passive and facilitated diffusion as candidate mechanisms for ERK1/2 nuclear translocation. The sizes of ERK2-GFP and ERK1/2-Dronpa are ~70 kDa. Diffusion into the nucleus is thought to be restricted to a size of 40–50 kDa (29). However, this value refers to a time window of less than 24 h after microinjection of the molecules of interest (30, 31). In our experiments the proteins were not introduced into the cells by microinjection but were expressed for at least 36 h from an expression vector introduced into the neurons by DNA transfection. During this time, diffusion through the nuclear pore could have occurred. Indeed, the passively diffusing MBP-Dronpa, which is 67 kDa in size, is localized to both the cytoplasm and the nucleus. Thus in hippocampal neurons, diffusion into the nucleus of proteins larger than 40–50 kDa occurs albeit at a very slow rate.

Our FRAP experiments revealed that ERK1/2-Dronpa was moving across the nuclear border significantly faster than MBP-Dronpa, indicating that ERK1/2-Dronpa enters the nucleus not by passive but by facilitated diffusion. This conclusion is further supported by the finding that nuclear translocation of ERK1/2-Dronpa, but not Dronpa (that because of its small size invades the nucleus by passive diffusion) was blocked by decreasing the temperature to 10 °C. Facilitated diffusion drops sharply in a nonlinear fashion with decreasing temperature, whereas passive diffusion is reduced in a linear manner (29, 32, 54). Temperature sensitivity was observed for the nuclear translocation of ERK1/2-Dronpa overexpressed in the absence of MEK1 as well as for stimulation-induced nuclear translocation of ERK1/2-Dronpa in neurons co-transfected with plasmids encoding ERK1/2-Dronpa and RFP-MEK1. Thus, facilitated diffusion appears to mediate nuclear translocation of ERK1/2-Dronpa, although some assistance from active import cannot be excluded.

Signal-induced Nuclear Translocation of ERK1/2—ERK1/2 fusion proteins, expressed either at low levels or co-expressed with RFP-MEK1, localized predominantly to the cytoplasm before stimulation and translocated to the nucleus upon induction of AP bursting or BDNF treatment. This distribution in stimulated and unstimulated neurons as well as the kinetics of nuclear translocation matched those of endogenous ERK1/2 proteins.

The rate of signal-induced nuclear translocation of ERK1/2-Dronpa appears to be independent of a nucleo-cytoplasmic concentration gradient for ERK1/2-Dronpa (see Fig. 6). There are several possible explanations for the persistence of nuclear translocation of ERK1/2 despite the absence of a concentration gradient; MEK1, which is actively exported from the nucleus in a CRM1-dependent manner, may function as a nucleus-to-cytoplasm shuttle for nuclear ERK1/2, which may get dephosphorylated within the nucleus; this generates a "sink" for nuclear extrusion of dephosphorylated ERK1/2 and may facilitate ongoing entry of phosphorylated ERK1/2 from the cytoplasm. Alternatively, the flux of phosphorylated ERK1/2 molecules through the nuclear pore occurs in both directions via facilitated diffusion. Thus a FRAP signal is generated by the ongoing exchange between nuclear and cytosolic pools of ERK1/2-Dronpa. Efflux from the nucleus increases following stimulation because of elevated nuclear ERK1/2 concentrations. When the distribution is equal in both compartments, influx and efflux are in balance. This nuclear/cytosolic exchange is absent when the concentration of ERK1/2 not bound to MEK1 is low as is the case in unstimulated cells. Consistent with the idea of continuously ongoing shuttling is the observation that the nuclear recovery rate after bleaching of freely diffusing Dronpa is very fast even in the absence of a nucleo-cytoplasmic concentration gradient (see Fig. 4*A*). This idea of ongoing shuttling independent of an active export mechanism is also supported by findings in NIH-3T3 cells (24).

Diffusion has also been suggested as the mechanism of ERK1/2 translocation into the nucleus in HEK-293 and NIH-3T3 cells (24, 27). However, in HEK-293 cells no difference was found in the mobility of ERK-YFP and YFP in the cytoplasm and across the nuclear membrane despite the accumulation of ERK-YFP to a 1.5–2 n/c ratio in steady state, which greatly exceeded that of YFP alone (27). In contrast, in NIH-3T3 cells GFP has been shown to move at a significantly faster speed than ERK2-GFP (24). Similarly, in hippocampal neurons, Dronpa moves much faster than ERK1/2-Dronpa in both the cytoplasm (dendrites) and across the nuclear membrane, and Dronpa and ERK1/2-Dronpa show an equivalent steady-state n/c ratio. The

differences in the results obtained in these studies may be due to cell type differences or differences in measurement sensitivities because of spatial restrictions. The geometry of neurons and the use of Dronpa allowed us to measure diffusion over 80 μm in dendrites as opposed to the 1 μm^2 analyzed in the HEK-293 cells (27).

The results of Costa *et al.* (24) in NIH-3T3 cells support our model of facilitated diffusion as a likely mechanism for nuclear translocation, although the precise spatial dynamics of ERK1/2 in NIH-3T3 cells are different from those in cultured hippocampal neurons.

Dendritic Trafficking of ERK1/2—Our experiments revealed that ERK1/2-Dronpa diffuses throughout the dendrites in a nondirectional manner and, unlike other proteins such as BDNF (55) or NF-κB (42), is not transported in a retrograde fashion toward the cell soma. Co-expression of RFP-MEK1 or induction of ERK1/2 phosphorylation did not affect the mode or kinetics of ERK1/2-Dronpa dendritic trafficking in agreement with findings in the cytoplasm of HEK-293 cells (27). MEK1-Dronpa and ERK1/2-Dronpa diffused slower in dendrites than an equivalently sized molecule, MBP-Dronpa. It is possible that the interaction of ERK1/2 and MEK1 with other proteins affects their trafficking in dendrites. MEK1 and ERK1/2, unlike MBP-Dronpa, are integrated into a protein kinase cascade and have upstream and downstream binding partners that might retard their diffusion.

Local ERK1/2 Signaling in Dendrites—Given diffusion-mediated movement of ERK1/2 in dendrites, the action of activated ERK1/2 is likely to be spatially restricted, and ERK1/2 activated at distal synapses may not reach the nucleus. Several ERK1/2 functions not involving signal propagation to the nucleus have been described. These include the regulation of α-amino-3-hydroxy-5-methyl-4-isoxazolepropionic acid receptor surface expression during synaptic plasticity (9) and the modulation (phosphorylation) of a dendritic Kv4.2 potassium channel subunit (56) that is involved in the control of neuronal excitability and nociception (57). ERK1/2 have also been implicated in the regulation of spine morphogenesis (58) and the control of local protein synthesis (59, 60). Thus, the predominant function of ERK1/2 in terminally differentiated neurons may be to modulate biochemical processes in the dendrites near the sites of ERK1/2 activation. A successful link to the regulation of transcription may require ERK1/2 activation within or near the cell soma.

Long Distance Signaling by ERK1/2-independent Mechanisms—If only somatic and peri-somatic pools of activated ERK1/2 can transmit signals across the nuclear border, how do distal synapses communicate with the nucleus? Several studies indicate that calcium itself can convert synaptic activity into a transcription-regulating nuclear signal (37, 61–63). Calcium transients initiated by synaptic activity and calcium entry into neurons through ligand- and/or voltage-gated calcium channels in the dendritic tree as well as the cell soma invade the nucleus within milliseconds of the stimulation (37, 63, 64). In brain slices, synaptic inputs at distances of more than 150 μm from the cell soma can generate robust calcium transients in the cell nucleus.[3] Nuclear calcium has emerged as an important activator of neuronal gene expression (61, 62). Acting via nuclear calmodulin and nuclear calcium/calmodulin-dependent protein kinases, nuclear calcium is both sufficient to stimulate phosphorylation of CREB on its activator site serine 133 and necessary for neuronal activity-induced gene transcription mediated by CREB and its co-activator CREB-binding protein (37, 65). Moreover, nuclear calcium signaling is critical for the transcription-dependent late phases of synaptic plasticity and learning (66) and for activity-dependent neuronal survival (40, 67). The slower invasion of the nucleus by activated ERK1/2 may complement the nuclear calcium signal to prolong and/or strengthen CREB/CREB-binding protein-mediated transcription (19, 68). Our findings, however, suggest that only pools of ERK1/2 activated in the soma or in the proximal dendrite are likely to contribute to nuclear signaling. Such a transcription-relevant ERK1/2 activation may be initiated by calcium entry through ligand- and/or voltage-gated calcium channels located in the cell soma and the proximal dendrites or by calcium release in the cell soma from intracellular calcium stores (64, 69, 70).

Conclusion—ERK1/2 movements within dendrites are signal-independent and occur by passive diffusion. The reach of a locally activated pool of ERK1/2 follows an exponential decay curve. Translocation to the nucleus only takes place after ERK1/2 activation and is mediated largely by facilitated diffusion. Because diffusion mediates and thus limits dendritic transport of ERK1/2, only ERK1/2 pools activated within or near the cell soma are likely to invade the nucleus and stimulate gene expression.

Acknowledgments—We thank Philip J. Stork, Atsushi Miyawaki, and Michiyuki Matsuda for generously supplying plasmids; Iris Bünzli-Ehret for preparing hippocampal cultures; and Dirk Görlich for advice and discussion.

REFERENCES

1. Nakamura, T., Sanokawa, R., Sasaki, Y., Ayusawa, D., Oishi, M., and Mori, N. (1996) *Oncogene* **13,** 1111–1121
2. Bading, H., and Greenberg, M. E. (1991) *Science* **253,** 912–914
3. Dolmetsch, R. E., Pajvani, U., Fife, K., Spotts, J. M., and Greenberg, M. E. (2001) *Science* **294,** 333–339
4. Thomas, G. M., and Huganir, R. L. (2004) *Nat. Rev. Neurosci.* **5,** 173–183
5. Deisseroth, K., Mermelstein, P. G., Xia, H., and Tsien, R. W. (2003) *Curr. Opin. Neurobiol.* **13,** 354–365
6. Akashi, M., and Nishida, E. (2000) *Genes Dev.* **14,** 645–649
7. Ji, R. R., Baba, H., Brenner, G. J., and Woolf, C. J. (1999) *Nat. Neurosci.* **2,** 1114–1119
8. Valjent, E., Corvol, J. C., Pages, C., Besson, M. J., Maldonado, R., and Caboche, J. (2000) *J. Neurosci.* **20,** 8701–8709
9. Zhu, J. J., Qin, Y., Zhao, M., Van Aelst, L., and Malinow, R. (2002) *Cell* **110,** 443–455
10. Gille, H., Kortenjann, M., Thomae, O., Moomaw, C., Slaughter, C., Cobb, M. H., and Shaw, P. E. (1995) *EMBO J.* **14,** 951–962
11. Treisman, R. (1992) *Trends Biochem. Sci.* **17,** 423–426
12. Janknecht, R., Ernst, W. H., and Nordheim, A. (1995) *Oncogene* **10,** 1209–1216

[3] C. Peter Bengtson and Hilmar Bading, unpublished data.

13. Derijard, B., Hibi, M., Wu, I. H., Barrett, T., Su, B., Deng, T., Karin, M., and Davis, R. J. (1994) *Cell* **76,** 1025–1037
14. Chen, R. H., Juo, P. C., Curran, T., and Blenis, J. (1996) *Oncogene* **12,** 1493–1502
15. Xing, J., Ginty, D. D., and Greenberg, M. E. (1996) *Science* **273,** 959–963
16. Blenis, J. (1993) *Proc. Natl. Acad. Sci. U. S. A.* **90,** 5889–5892
17. Arthur, J. S., Fong, A. L., Dwyer, J. M., Davare, M., Reese, E., Obrietan, K., and Impey, S. (2004) *J. Neurosci.* **24,** 4324–4332
18. Sindreu, C. B., Scheiner, Z. S., and Storm, D. R. (2007) *Neuron* **53,** 79–89
19. Hardingham, G. E., Arnold, F. J., and Bading, H. (2001) *Nat. Neurosci.* **4,** 565–566
20. Howe, C. L., and Mobley, W. C. (2005) *Curr. Opin. Neurobiol.* **15,** 40–48
21. Delcroix, J. D., Valletta, J. S., Wu, C., Hunt, S. J., Kowal, A. S., and Mobley, W. C. (2003) *Neuron* **39,** 69–84
22. Reynolds, A. J., Hendry, I. A., and Bartlett, S. E. (2001) *Neuroscience* **105,** 761–771
23. Adams, J. P., and Dudek, S. M. (2005) *Nat. Rev. Neurosci.* **6,** 737–743
24. Costa, M., Marchi, M., Cardarelli, F., Roy, A., Beltram, F., Maffei, L., and Ratto, G. M. (2006) *J. Cell Sci.* **119,** 4952–4963
25. Khokhlatchev, A. V., Canagarajah, B., Wilsbacher, J., Robinson, M., Atkinson, M., Goldsmith, E., and Cobb, M. H. (1998) *Cell* **93,** 605–615
26. Adachi, M., Fukuda, M., and Nishida, E. (1999) *EMBO J.* **18,** 5347–5358
27. Burack, W. R., and Shaw, A. S. (2005) *J. Biol. Chem.* **280,** 3832–3837
28. Matsubayashi, Y., Fukuda, M., and Nishida, E. (2001) *J. Biol. Chem.* **276,** 41755–41760
29. Talcott, B., and Moore, M. S. (1999) *Trends Cell Biol.* **9,** 312–318
30. Paine, P. L., Moore, L. C., and Horowitz, S. B. (1975) *Nature* **254,** 109–114
31. Peters, R., Lang, I., Scholz, M., Schulz, B., and Kayne, F. (1986) *Biochem. Soc. Trans.* **14,** 821–822
32. Kose, S., Imamoto, N., Tachibana, T., Shimamoto, T., and Yoneda, Y. (1997) *J. Cell Biol.* **139,** 841–849
33. Gorlich, D., and Kutay, U. (1999) *Annu. Rev. Cell Dev. Biol.* **15,** 607–660
34. Ando, R., Mizuno, H., and Miyawaki, A. (2004) *Science* **306,** 1370–1373
35. Arnold, F. J., Hofmann, F., Bengtson, C. P., Wittmann, M., Vanhoutte, P., and Bading, H. (2005) *J. Physiol.* (*Lond.*) **564,** 3–19
36. Hardingham, G. E., Chawla, S., Cruzalegui, F. H., and Bading, H. (1999) *Neuron* **22,** 789–798
37. Hardingham, G. E., Arnold, F. J., and Bading, H. (2001) *Nat. Neurosci.* **4,** 261–267
38. Nguyen, P. V., Abel, T., and Kandel, E. R. (1994) *Science* **265,** 1104–1107
39. Morris, R. G. (1989) *J. Neurosci.* **9,** 3040–3057
40. Zhang, S. J., Steijaert, M. N., Lau, D., Schutz, G., Delucinge-Vivier, C., Descombes, P., and Bading, H. (2007) *Neuron* **53,** 549–562
41. Thomas, D., Tovey, S. C., Collins, T. J., Bootman, M. D., Berridge, M. J., and Lipp, P. (2000) *Cell Calcium* **28,** 213–223
42. Wellmann, H., Kaltschmidt, B., and Kaltschmidt, C. (2001) *J. Biol. Chem.* **276,** 11821–11829
43. Shibasaki, F., Price, E. R., Milan, D., and McKeon, F. (1996) *Nature* **382,** 370–373
44. Fukuda, M., Gotoh, I., Gotoh, Y., and Nishida, E. (1996) *J. Biol. Chem.* **271,** 20024–20028
45. Fukuda, M., Gotoh, Y., and Nishida, E. (1997) *EMBO J.* **16,** 1901–1908
46. Horgan, A. M., and Stork, P. J. (2003) *Exp. Cell Res.* **285,** 208–220
47. Horiuchi, K. Y., Scherle, P. A., Trzaskos, J. M., and Copeland, R. A. (1998) *Biochemistry* **37,** 8879–8885
48. Fujioka, A., Terai, K., Itoh, R. E., Aoki, K., Nakamura, T., Kuroda, S., Nishida, E., and Matsuda, M. (2006) *J. Biol. Chem.* **281,** 8917–8926
49. Boos, W., and Shuman, H. (1998) *Microbiol. Mol. Biol. Rev.* **62,** 204–229
50. Ribbeck, K., and Gorlich, D. (2002) *EMBO J.* **21,** 2664–2671
51. Stewart, M., Baker, R. P., Bayliss, R., Clayton, L., Grant, R. P., Littlewood, T., and Matsuura, Y. (2001) *FEBS Lett.* **498,** 145–149
52. Impey, S., Obrietan, K., Wong, S. T., Poser, S., Yano, S., Wayman, G., Deloulme, J. C., Chan, G., and Storm, D. R. (1998) *Neuron* **21,** 869–883
53. Osawa, M., Itoh, S., Ohta, S., Huang, Q., Berk, B. C., Marmarosh, N. L., Che, W., Ding, B., Yan, C., and Abe, J. (2004) *J. Biol. Chem.* **279,** 29691–29699
54. Harootunian, A. T., Adams, S. R., Wen, W., Meinkoth, J. L., Taylor, S. S., and Tsien, R. Y. (1993) *Mol. Biol. Cell* **4,** 993–1002
55. Adachi, N., Kohara, K., and Tsumoto, T. (2005) *BMC Neurosci.* **6,** 42
56. Yuan, L. L., Adams, J. P., Swank, M., Sweatt, J. D., and Johnston, D. (2002) *J. Neurosci.* **22,** 4860–4868
57. Hu, H. J., Carrasquillo, Y., Karim, F., Jung, W. E., Nerbonne, J. M., Schwarz, T. L., and Gereau, R. W. T. (2006) *Neuron* **50,** 89–100
58. Futter, M., Uematsu, K., Bullock, S. A., Kim, Y., Hemmings, H. C., Jr., Nishi, A., Greengard, P., and Nairn, A. C. (2005) *Proc. Natl. Acad. Sci. U. S. A.* **102,** 3489–3494
59. Sweatt, J. D. (2004) *Curr. Opin. Neurobiol.* **14,** 311–317
60. Thiels, E., and Klann, E. (2001) *Rev. Neurosci.* **12,** 327–345
61. Hardingham, G. E., Chawla, S., Johnson, C. M., and Bading, H. (1997) *Nature* **385,** 260–265
62. Bading, H. (2000) *Eur. J. Biochem.* **267,** 5280–5283
63. Raymond, C. R., and Redman, S. J. (2006) *J. Physiol.* (*Lond.*) **570,** 97–111
64. Zhao, M., Adams, J. P., and Dudek, S. M. (2005) *J. Neurosci.* **25,** 7032–7039
65. Chawla, S., Hardingham, G. E., Quinn, D. R., and Bading, H. (1998) *Science* **281,** 1505–1509
66. Limback-Stokin, K., Korzus, E., Nagaoka-Yasuda, R., and Mayford, M. (2004) *J. Neurosci.* **24,** 10858–10867
67. Soriano, F. X., Papadia, S., Hofmann, F., Hardingham, N. R., Bading, H., and Hardingham, G. E. (2006) *J. Neurosci.* **26,** 4509–4518
68. Wu, G. Y., Deisseroth, K., and Tsien, R. W. (2001) *Proc. Natl. Acad. Sci. U. S. A.* **98,** 2808–2813
69. Frey, U., and Morris, R. G. (1997) *Nature* **385,** 533–536
70. Dudek, S. M., and Fields, R. D. (2002) *Proc. Natl. Acad. Sci. U. S. A.* **99,** 3962–3967